Original article
DOI: https://doi.org/10.18721/JPM.19204

SUPERCOMPUTER SIMULATION OF THE DYNAMICS OF OLIGOMERS OF A NUMBER OF AMINO ACIDS (Gly, Ala, Trp, Val) IN AN INFRARED ELECTROMAGNETIC FIELD

M. A. Baranov✉, *O. Yu. Tsybin*

Peter the Great St. Petersburg Polytechnic University,
St. Petersburg, Russia

✉ baranovma1993@gmail.com

Abstract. Supercomputer simulation of several amino acid oligomers using the molecular dynamics method has made it possible for the first time to identify a complex of characteristics of both intrinsic intramolecular local vibrations, or normal modes, and forced vibrations when specifying an alternating electric field in the IR frequency range. Amplitude-time dependences of energy and electric dipole moment were obtained for oligomers of Gly, Ala, Trp, Val amino acids, the Fourier transform of which revealed their frequency spectra. The type of solvent model was shown to significantly affect the position of spectral peaks because of variations in local interactions and system dynamics. The interpretation of the obtained patterns made it possible to propose a non-contradictory model that satisfied the fundamental physical concepts of the intramolecular and intermolecular dynamics of groups of biomolecules. The model allows for intramolecular interactions of normal local vibrations, including those of the Fermi resonance type.

Keywords: molecular dynamics, simulation, amino acid, biomolecular electronics

Citation: Baranov M. A., Tsybin O. Yu., Supercomputer simulation of the dynamics of oligomers of a number of amino acids (Gly, Ala, Trp, Val) in the infrared electromagnetic field, St. Petersburg State Polytechnical University Journal. Physics and Mathematics. 19 (2) (2026) 39–56. DOI: https://doi.org/10.18721/JPM.19204

This is an open access article under the CC BY-NC 4.0 license (https://creativecommons.org/licenses/by-nc/4.0/)

Научная статья
УДК 53.093, 53.096, 57.031, 57.033, 57.038
DOI: https://doi.org/10.18721/JPM.19204

СУПЕРКОМПЬЮТЕРНОЕ МОДЕЛИРОВАНИЕ ДИНАМИКИ ОЛИГОМЕРОВ РЯДА АМИНОКИСЛОТ (Gly, Ala, Trp, Val) В ЭЛЕКТРОМАГНИТНОМ ПОЛЕ ИНФРАКРАСНОГО ДИАПАЗОНА

М. А. Баранов✉, *О. Ю. Цыбин*

Санкт-Петербургский политехнический университет Петра Великого,
Санкт-Петербург, Россия

✉ baranovma1993@gmail.com

Аннотация. Суперкомпьютерное моделирование методом молекулярной динамики ряда олигомеров аминокислот позволило впервые выявить для таких частиц особенности комплекса характеристик как собственных внутримолекулярных локальных колебаний (нормальных мод), так и вынужденных колебаний в растворе

© Baranov M. A., Tsybin O. Yu., 2026. Published by Peter the Great St. Petersburg Polytechnic University.

при задании электромагнитного поля в дальнем и среднем ИК-диапазонах, а также различных алгоритмов структуры растворителя. Для олигомеров аминокислот Gly, Ala, Trp, Val и их групп получены амплитудно-временные зависимости энергии и электрического дипольного момента, Фурье-преобразованием которых выявлены спектры частот. Впервые обнаружены и вычислены смещения спектральных пиков, вызванные различиями алгоритмов задания структуры растворителя. Интерпретация полученных закономерностей позволила предложить непротиворечивую модель, удовлетворяющую фундаментальным физическим представлениям о внутримолекулярной и межмолекулярной динамике групп биомолекул. Эта модель допускает внутримолекулярные взаимодействия нормальных локальных колебаний, в том числе по типу Ферми-резонанса.

Ключевые слова: молекулярная динамика, компьютерное моделирование, аминокислота, биомолекулярная электроника

Ссылка для цитирования: Баранов М. А., Цыбин О. Ю. Суперкомпьютерное моделирование динамики олигомеров ряда аминокислот (Gly, Ala, Trp, Val) в электромагнитном поле инфракрасного диапазона // Научно-технические ведомости СПбГПУ. Физико-математические науки. 2026. Т. 19. № 2. С. 39–56. DOI: https://doi.org/10.18721/JPM.19204

Статья открытого доступа, распространяемая по лицензии CC BY-NC 4.0 (https://creativecommons.org/licenses/by-nc/4.0/)

Introduction

Forced vibrational processes in biomolecules, driven by external electromagnetic fields, are of considerable importance for life sciences, medicine, microelectronics, nanotechnology, and experimental spectroscopy [1–13]. Computational analysis of the time-dependent total dipole moment (summed over all molecular charges) in the absence of an applied field revealed the sub-picosecond dynamics of intrinsic biomolecular vibrations [14, 15]. The intrinsic vibrational frequencies correspond to local normal modes and delocalized collective motions spanning the terahertz (THz) to infrared (IR) range. Molecular dynamics simulation computing the time-dependent total dipole moment under an applied electromagnetic field makes it possible to determine molecular conformations and IR absorption spectra of forced vibrations, yielding substantial scientific and applied results in modern bio- and nanophysics [10, 16–25]. For instance, molecular dynamics simulations were performed for monomers, dimers, and protofibrils of Aβ42 in the THz range, and the applicability of the method to the mid- and far-infrared ranges was also confirmed [20]. It was shown that Newtonian force-field mechanics is a valid approach in molecular dynamics for the mid- and far-infrared ranges, alongside quantum-mechanical calculations [17, 20, 21, 23, 24, 26–28]. Comparisons of molecular dynamics studies in these frequency ranges yield reasonably close agreement between the calculated spectral characteristics and experimental or theoretical data for both intrinsic and forced vibrations [6, 21–23].

For example, the assignments of the most intense intrinsic vibrations at the calculated frequencies (wavenumbers, cm^{-1}) are given for amino acid solutions:

1100, 1519, 1652, 3018, 3322, 3364, 3362 for alanine (Ala);
927, 1060, 1542, 1643, 3210, 3322, 3364, 3479 for glycine (Gly);
1048, 1533, 1640, 3030, 3325, 3361, 3479, 3663 for valine (Val);
784, 1403, 1495, 1536, 1646, 2917, 3325, 3562, 3766 for tryptophan (Trp).

These results are in agreement with theoretical and experimental data reported previously, although the extent of this agreement has not been quantified [26, 28].

© Баранов М. А., Цыбин О. Ю., 2026. Издатель: Санкт-Петербургский политехнический университет Петра Великого.

According to the established view, spectral components above roughly 200–800 cm^{-1} correspond to local intramolecular vibrations (normal modes), while those below this range are collective delocalized vibrations. The assignment of local oscillator bands to normal modes and their frequencies was discussed in numerous sources, for example, in [26].

The spectral window from 2600 to 900 cm^{-1} is reported in [29]. Nine characteristic vibrational bands (amides A, B, I, II, ..., VII) are prominent in the IR spectrum, with amides I and II falling between 1600–1700 cm^{-1} and 1500–1600 cm^{-1}, respectively. The unperturbed C=O stretching vibration (amide I) has a frequency of 1688 cm^{-1}; the corresponding spectral band shifts in the presence of water or other solvents and also depends on conformation. The N–H bending vibration (Amide II) occurs in the wavenumber range of 1530–1580 cm^{-1}. The Cα–N stretching vibration (Amide III) falls within the range of 1200–1340 cm^{-1}. The resonant field frequencies (fundamental frequencies of the square wave at 3335.66 and 1042.37 cm^{-1}) coincide with specific intrinsic local vibrations (asymmetric N–H stretching of Amide A and C–N stretching, respectively).

Recent advances in molecular dynamics yielded new supercomputer simulation results describing the dynamics of increasingly complex protein molecules under electric fields with various polarizations and modulations in the THz and IR ranges [30–33]. Oligomers are attracting growing attention as key functional units that enable proteins to initiate allostery and cooperativity [14, 15, 34–37].

The vibrational dynamics of oligomers driven by electromagnetic fields of different polarizations and time profiles was simulated for the first time over a range of wavenumbers, particularly in the far- and mid-infrared ranges [25].

The goal of this supercomputer study is to refine the analysis of forced vibrations of oligomers and their aggregates in solution, which is essential for advancing fundamental biological and biophysical understanding, as well as for a range of current and emerging applications.

Computational approach and validation

The computational approach we adopted relies on a methodology for supercomputer simulation of molecular dynamics that has already proven to be highly efficient and reliable [25, 29, 38–41].

The techniques previously developed for single molecules were also applied here to oligomers and their assemblies.

The dynamic simulations of molecular complexes were performed using the RSC Tornado cluster at the Polytechnic Supercomputer Center of Peter the Great St. Petersburg Polytechnic University, as described in detail in our previous work [33]. The cluster, with a peak performance of 10^{15} flops, comprises 668 dual-processor nodes (Intel Xeon E5-2697 *v*33), 56 of which are equipped with two NVIDIA K40 accelerators. This configuration allows generating, within a reasonable computation time, extensive databases of the time-dependent total dipole moment with trajectory durations up to 40 ns and a minimum sampling interval of 1 fs, thereby providing high resolution in the Fourier spectra over the far- and mid-infrared frequency ranges. The software suite included Avogadro, Visual Molecular Dynamics (VMD), and NAMD, along with additional custom Python scripts. The Packmol tool was used to place oligomers in groups of $p = 1, 2, ..., 20$ particles within a cubic water box with a side length of 70 E. Initial coordinate files for the Gly, Ala, Trp and Val oligomers in aqueous solution were generated using Avogadro. The results presented below are primarily from simulations of polyAlaN oligomers (initially modelled as α-helices) with different numbers of amino acid residues $N = 18$,... ,2 ,1. The VMD software was used to generate structural files based on the topology of molecular bonds, add water molecules and salt ions, visualize molecular systems, calculate the energy and dipole moments of conformationally flexible molecules. Newton's equations of motion were solved for each atom of the system, atomic coordinates, force field parameters, system temperature, pressure, etc. were determined at each time step. The time-dependent total dipole moment $\mu(t)$ was then computed from the instantaneous coordinates and velocities of the charged particles by summing the displacement vectors of each charge at each time step.

The change in the partial dipole moment $\Delta\mu_{n,j}$ at the jth time step of duration Δt corresponds to the spatial displacement of charge q_n by the vector $\Delta\mathbf{r}_{n,j}$:

$$\Delta\mu_{n,j} = q_n \Delta \mathbf{r}_{n,j} = q_n \left[r_{n,j} - r_{n,j-1} \right].$$

The time-dependent total dipole moment $\mu(t)$ was then obtained by summing the partial moments over all charges in the oligomer solution:

$$\mu(t) = \sum_j \sum_n^N q_n \Delta \mathbf{r}_{n,j}, \quad (1)$$

where N is the total number of charges.

The time series of the instantaneous total dipole moment, $\mu(t)$, represents a superposition of the local vibrational motions of all charged atoms within the molecule.

The wavenumber spectrum of these vibrational motions was obtained by Fourier transformation of the time-dependent total dipole moment, both for each individual oligomer and for the entire assembly of particles in the simulation cell. The algorithm for computing the time series relies on the independence of the fluctuations of the total dipole moment (1) from the origin of the displacement vectors $\Delta \mathbf{r}_{n,j}$. High resolution in the characteristic frequencies of the studied part of the Fourier spectrum was achieved due to its numerical equality to the ratio of the duration of the amplitude-time realization to the oscillation period.

The Fourier method employed here has the advantage of reproducing all spectral components within a specified wavenumber range, including higher harmonics and combination bands. The range is limited by half the sampling frequency but can be extended using the computational resources of the supercomputer.

An applied electric field induces charge displacements at characteristic IR frequencies and a polarization response altering the components and magnitude of the dipole moment. To ensure the most informative study, three types of electromagnetic fields were specified with plane spatial polarization along the coordinate axes (x,y,z), with components [E,0,0] and amplitudes from 0.01 to 0.50 V/nm:

a harmonic electric field,

a periodic sequence of unipolar rectangular pulses,

a symmetric square wave.

The square wave was chosen because it combines the properties of periodic pulse sequences and is of practical interest for microelectronics, particularly for controlled switching of molecular states and for probing anharmonic molecular dynamics. The feasibility and effectiveness of a square-wave electric field with a fundamental frequency in the IR range were tested and validated in several studies [14, 15, 23–25]. A similar square-wave electric field was used in molecular dynamics simulations of liquid water in the 20–500 GHz frequency range [40].

The strength of the local electric field acting on the charges within the molecule was varied over a wide range, from 0.004 to 0.400 V/nm. As in our previous works and in studies by other authors, the time dependence of the vibrational amplitudes was linear and did not lead to molecular fragmentation. Indeed, such fields exist only in the microscopic region near a charge and correspond to typical atomic intramolecular fields. This approach does not require comparison with macroscopic fields, which have different energy characteristics [42–44].

Based on the obtained data for the intrinsic vibrational spectra of oligomers, we applied the electric field $E(t)$ at a set of resonant frequencies corresponding to the following fundamental wavenumbers (in cm^{-1}):

5555, 4167, 3333, 1667, 1515, 1111, 1042, 980 and 200.

The energy characteristics corresponding to these wavenumbers are shown in Fig. 1.

The time evolution of the kinetic and potential energies of the particles and the system as a whole was computed simultaneously with the time-dependent dipole moment.

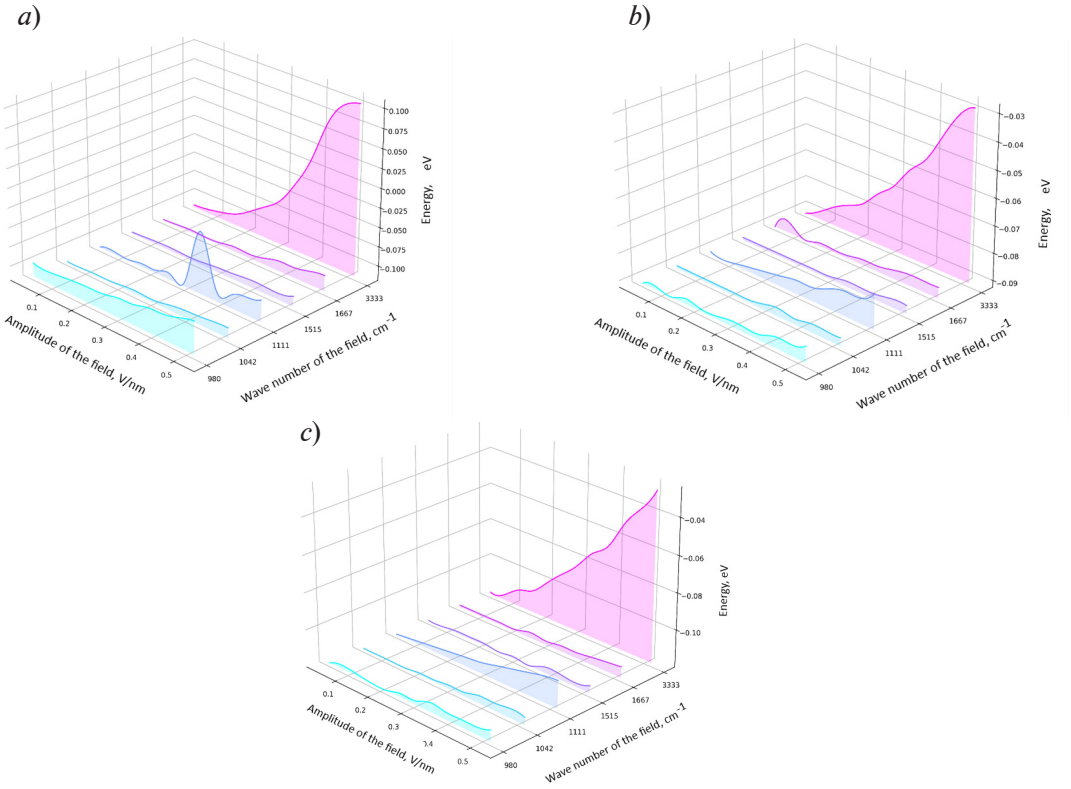


Fig. 1. Typical potential energy characteristics of Ala (*a*), Gly (*b*), Trp (*c*) molecules in aqueous solution obtained with an explicit solvent model. The figure shows 3D plots of energy as a function of square-wave amplitude of the electric field at selected wavenumbers (WN). Temperature: 298 K, time step: 5 fs

The most pronounced dependence on the strength of the alternating electric field was observed at the wavenumber 3333 cm^{-1}, corresponding to the asymmetric N–H stretching vibrations (Amide A) (see Fig. 1,*a*). This may also be related to preferential localization of vibrations in hydrogen-bond networks. The molecular energy at resonance depended to a greater extent on the applied field strength and to a lesser extent (or not at all) on the trajectory duration. The potential energy remained nearly constant in the field strength range from approximately 0.01 to 0.50 V/nm over the time interval from 0 to 510 ps for Gly and Trp, showing a more complex dependence for Ala, presumably due to the larger side chain (see Fig. 1,*b*).

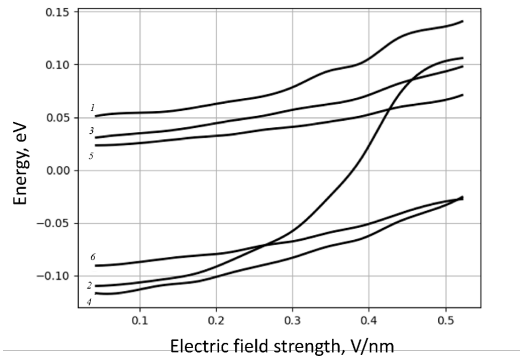


Fig. 2. Potential and kinetic energies of diphenyl-L-alanine (*1*, *2*), tryptophan (*3*, *4*), and glycine (*5*, *6*) in aqueous solution as function of field strength at t = 500 ps
Fundamental wavenumber of electric field: 3333 cm^{-1}

Fig. 2 shows the potential and kinetic energies of diphenyl-L-alanine, tryptophan, and glycine in aqueous solution as functions of the field strength at a fixed time t= 500 ps. Fundamental wavenumber of electric field: 3333 cm^{-1}. Notably, there is a linear increase in energy from very small field strengths at the fundamental frequency of 3333 cm^{-1} up to about 0.4 V/nm for glycine and tryptophan, and up to 0.2 V/nm for diphenyl-*L*-alanine. At other characteristic frequencies (e.g., 980 and 200 cm^{-1}), both types of energy were nearly independent of the field strength, which is consistent with the data in Fig. 1,*a*.

Shifts in the spectral peaks along the wavenumber scale were observed, depending on the algorithms chosen for local interactions and system dynamics. Specifically, the virtual molecular systems differed in the way water (solvent) was added: either as an implicit solvent or as an explicit solvent (with water molecules added), i.e., using the coarse-grained model [45].

In the latter case, the volume and complexity of computations increase significantly because it is necessary to set the parameters and states of the water molecules, the size of the water box, etc. The generalized Born implicit solvent (GBIS) method was used for the former case. It is a fast but approximate method for calculating molecular electrostatics in a solvent, described by the Poisson–Boltzmann equation, which models water as a dielectric continuum:

$$\nabla \times \left[\varepsilon(\mathbf{r})\nabla\varphi(\mathbf{r})\right] = -\rho^{f}(\mathbf{r}) - \sum_{i} c_{i}^{\infty} z_{i} e_{0} \exp\left[\frac{-z_{i} e_{0}\varphi(\mathbf{r})}{k_{\mathrm{B}} T}\right], \quad (2)$$

where $\varepsilon(\mathbf{r})$ is the dielectric permittivity of the medium, φ is the electric potential, $\rho^{f}(\mathbf{r})$ is the charge density in the medium, c^{∞}_{i} is the concentration of the ith ion at infinity, z_i is the valence of the ith ion, k_{B} is the Boltzmann constant, T is the temperature.

This method allows simulating atomic structures without including explicit water, i.e., without adding hydrogen and oxygen atoms and without computing their coordinates. Using an implicit solvent significantly accelerates the simulations and greatly reduces the size of the output files (roughly in a 1 : 50 GB ratio), which was a key factor in this study.

Amino acid molecules were placed in a periodic system with a cubic water cell (with a side length of 70 E, independent of the molecular sizes). The distance from the outermost molecule to the cell boundary was 15 E. Solvation of molecules was simulated by the TIP3W water model, corresponding to three atoms of the water molecule at three interaction points. Such models provide high computational efficiency and are used in many applications for molecular dynamics simulation. The chosen water model was also used with the CHARMM force field. The difference lies in the Lennard–Jones parameters: unlike TIP3, the CHARMM version of the model assigns these parameters to hydrogen atoms in addition to the oxygen parameters in the water molecule [46, 47]. Many similar studies used this water model, but the frequency shifts of intrinsic vibrations associated with different algorithms were not discussed previously [48, 49].

Simulation results

Fig. 3 shows the spectral characteristics of water in the periodic system of cubic cells, computed in this paper using the explicit solvent model; the ranges of intrinsic vibrations of water molecules known from the literature are also shown for comparison [50].

The Fourier spectrum of the electric dipole moment of water molecules was calculated using the VMD IR Spectral Density Calculator plugin; the duration of the amplitude-time realization was 20 ns.

Analyzing the spectra in Fig. 3, we can conclude that the vibrational bands of water molecules are close to the positions of the intrinsic vibrational peaks of biomolecules [20, 30, 31, 33]. The resonant spectral effects of forced vibrations under an applied electric field, observed in the total dipole moments of oligomer assemblies, are similar in energy characteristics to those found for single amino acid molecules [20, 33] as well as for dimers, trimers, and other peptides [51, 52].

The Fourier spectra of the intrinsic intramolecular vibrational bands of polyAlaN oligomers were qualitatively similar for different N (N = 1, 2, ..., 18) and for different numbers p (p = 1, 2, ..., 10) of such oligomers in the water box, but they also exhibited several quantitative features. Fig. 4 shows the typical overview and selected window spectra of polyAla12 oligomers, derived from the time-dependent total dipole moment reflecting the intrinsic vibrational motions of the molecules. The spectra were obtained with a trajectory duration of 2 ns, time window of 510 ps, and a time step of 5 fs (T = 298 K).

Comparing the overview Fourier spectra of intrinsic vibrations for single polyAla12 oligomers (p = 1) and for their assemblies with p = 10 (see Fig. 4), we found that the set of spectral components was virtually identical. However, a change in the spectral components was

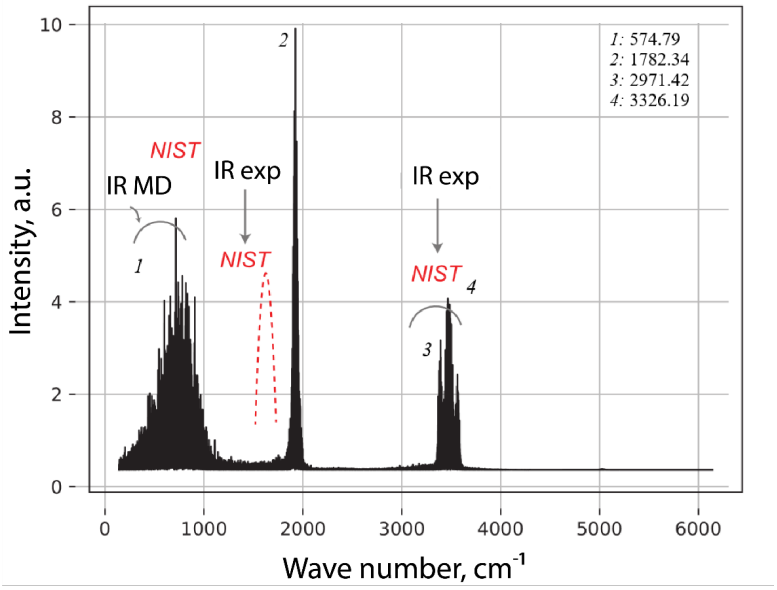


Fig. 3. Fourier spectra of time-dependent dipole moment of water molecules: IR MD corresponds to results obtained with the VMD IR Spectral Density Calculator plugin (t = 1 ns, f_D = 200 THz); IR exp NIST corresponds to the experimental results from the NIST database [48]
The wavenumbers (cm^{-1}) of spectral bands *1–4* are given in the legend

observed as the number of oligomers increased: the structure with two peaks in the center at 3313.5 and 3358.1 cm^{-1} transformed into a structure with two peaks at 3277 and 3394.4 cm^{-1}. This change likely indicates dipole–dipole interactions between oligomers in the assembly. A similar evolution of spectral components was reproduced for other values of the parameters N and p. The differences observed between the typical spectral windows from the overview spectra of polyAla12 oligomer assemblies (see Fig. 4) are likely due to phonon–phonon coupling of local vibrations, as well as to collective mechanisms forming spectral components in the molecular assembly.

The Fourier spectra of forced vibrations for polyAla18 oligomers (p = 1) were calculated from the total dipole moment, with a trajectory duration of 2 ns, under an applied symmetric square-wave electric field. The square-wave amplitude was varied over two orders of magnitude, from 0.004 to 0.400 V/nm, corresponding to local atomic fields within the molecule. The fundamental harmonics showed essentially the same behavior and patterns at different vibrational frequencies with varying excitation parameters. Fig. 5 shows the typical overview spectra of forced vibrations for polyAla18 oligomers at p = 1, computed from the total dipole moment, with a trajectory duration of 2 ns, under an applied symmetric square-wave electric field with a peak-to-peak amplitude of 0.4 V/nm at different fundamental wavenumbers.

Spectra with similar characteristics were obtained at lower fields in the range of 0.01–0.400 V/nm for all three types of electric field.

Comparing the spectra of forced vibrations (see Fig. 5) and intrinsic vibrations, we found that field excitation at wavenumbers of 5555 and 4167 cm^{-1}, as well as at other wavenumbers in the region above the frequencies of intrinsic local vibrations, did not cause any noticeable rearrangement of the spectral components of oligomers for different N(N = 1, 2, ..., 18). When the excitation frequency coincided with an intrinsic local vibration frequency, for example at wavenumbers (in cm^{-1}) of 3333, 1111, 1042, and 980, a strong rearrangement of the spectral components was observed, consistent with resonant pumping of forced vibrations (see Fig. 4). This result is likely due to corresponding changes in the conformational structure and in the total dipole moment. Indeed, the frequency dependences obtained for the time-averaged total dipole moment of polyAla18 oligomers for different values of p at a field strength E= 0.4 V/nm were consistent with this interpretation.

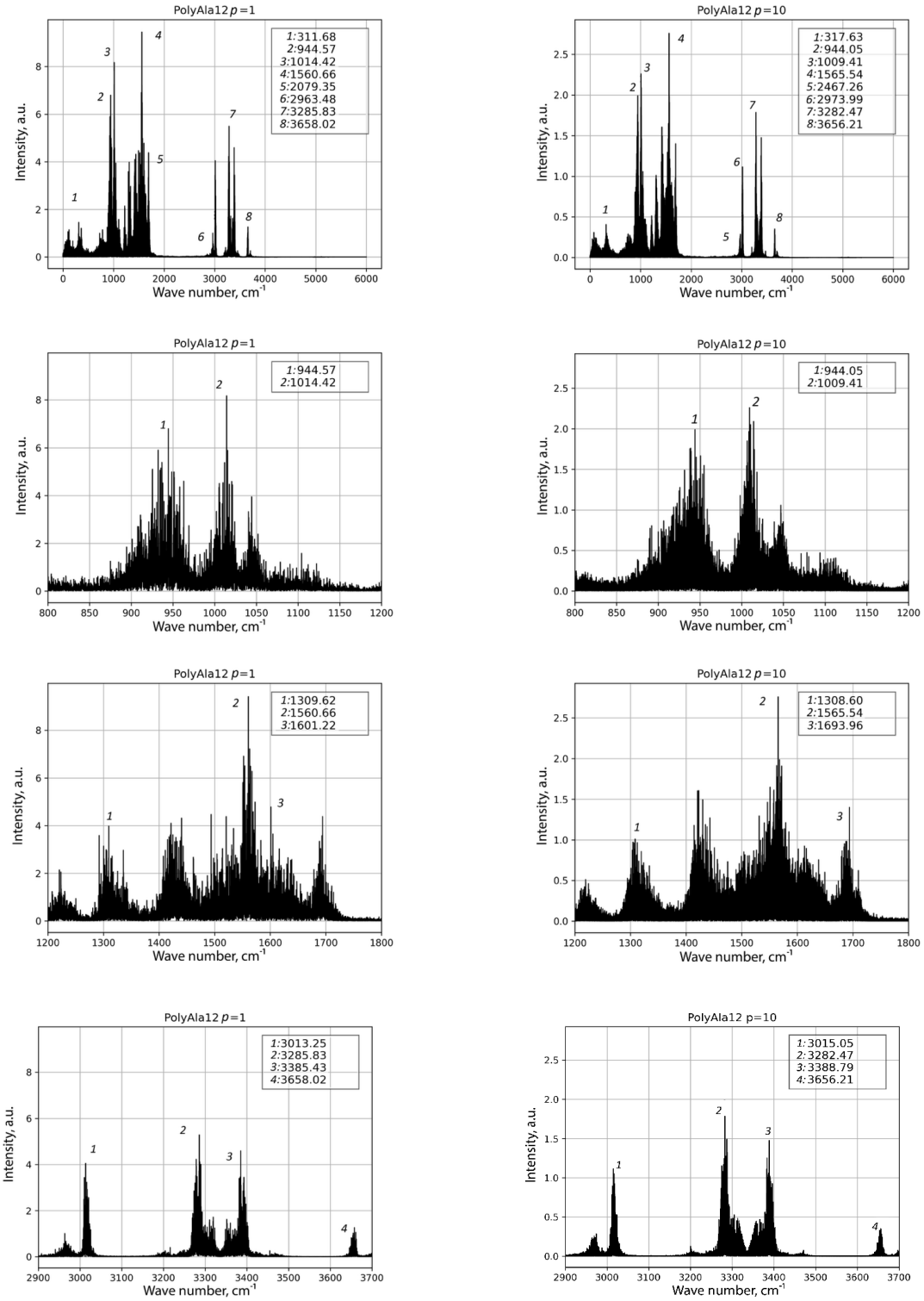
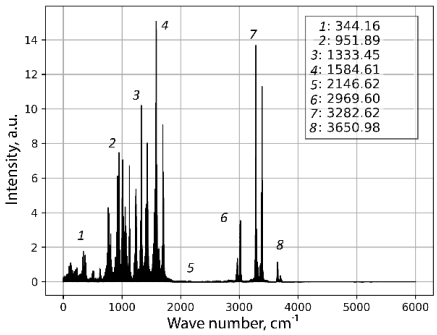
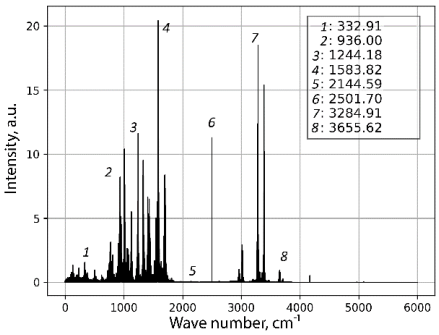


Fig. 4. Overview vibrational spectra of polyAla12 oligomers, computed from the total dipole moment. Selected spectral windows are shown for different numbers p of oligomers
The wavenumbers (cm^{-1}) of spectral bands are given in the legends

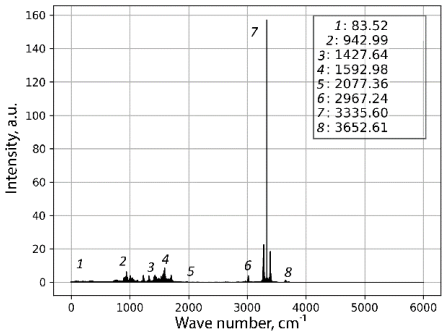
a) WN = 5555 cm^{-1}



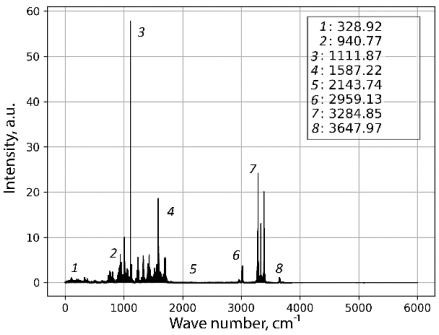
b) WN =4167 cm^{-1}



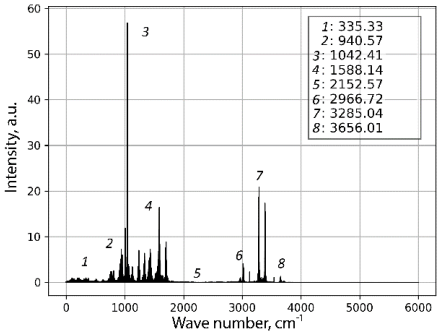
c) WN = 3333 cm^{-1}



d) WN =1111 cm^{-1}



e) WN = 1042cm^{-1}



f) WN = 980cm^{-1}

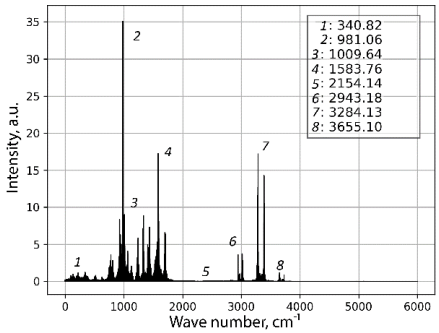


Fig. 5. Fourier spectra of forced vibrations
for polyAla18 oligomers (p = 1), computed from the total dipole moment,
with trajectory duration of 2 ns, under an applied symmetric square-wave electric field
(peak-to-peak amplitude of 0.4 V/nm), at different fundamental wavenumbers (WN)

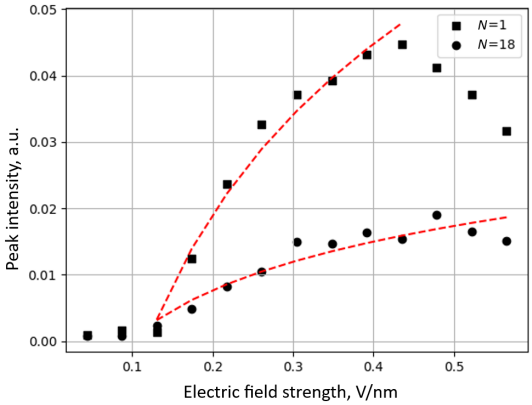


Fig. 6. Resonance peak intensity of polyAlaN molecules at $N = 1$ and $N = 18$ ($p = 1$) as a function of electric field strength under square-wave excitation at WN = 3333 cm^{-1}

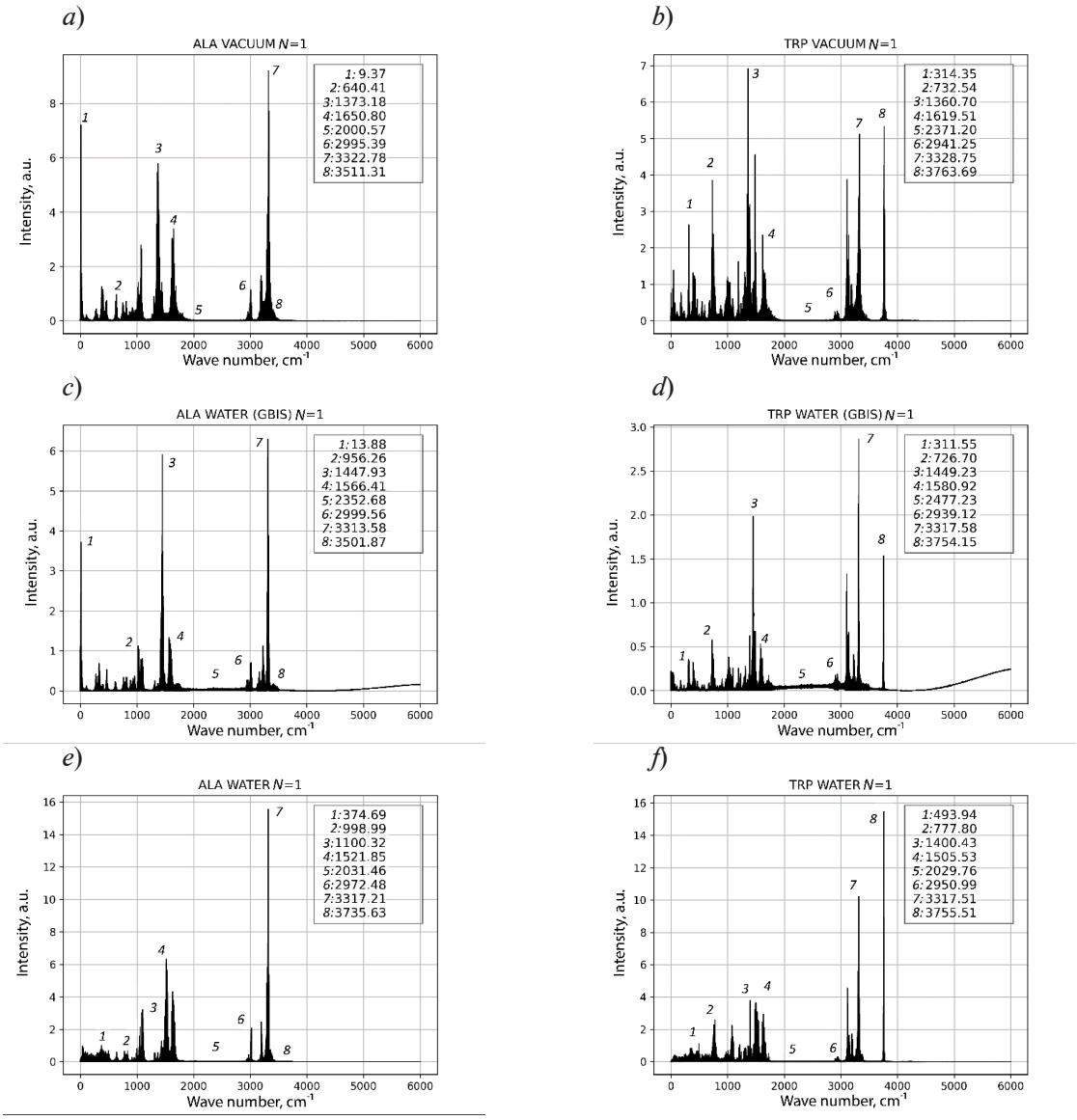


Fig. 7. Simulated Fourier spectra of time-dependent dipole moment for Ala and Trp molecules ($t = 1$ ns) in different environments: Ala in vacuum (*a*); Trp in vacuum (*b*); Ala with GBIS (*c*); Trp with GBIS (*d*); Ala in explicit water solvent (*e*); Trp in explicit water solvent (*f*)

Fig. 6 shows the intensities of the peaks in the resonant spectral bands of polyAlaN molecules at $N = 1$, $N = 18$ and $p = 1$ as a function of the electric field strength under square-wave excitation at a fundamental wavenumber of 3333 cm^{-1}. A nearly linear relationship was observed between the resonance peak intensities and the electric field strength in the region of very small field amplitudes. This linear region extends up to the maximum intensities of the resonant spectral bands, when the field amplitude reaches about 0.4 V/nm, which is consistent with the results known from the literature [53, 54].

The spectral line intensities at different excitation frequencies either remained virtually unchanged or increased linearly with increasing field strength over the given range.

Fig. 7 shows the spectral characteristics of the amplitude-time realization of the electric dipolemoments of Ala and Trp molecules simulated for vacuum conditions and various water-solvent models. The differences revealed in the spectral characteristics, discussed below, allowed us to formulate and justify some significant additions to the description of the vibrational properties of molecules.

Discussion

The results presented above allow analyzing the dynamic properties of the considered set of oligomers in the IR range. Comparing the overview Fourier spectra of intrinsic vibrations for single oligomers and for their assemblies, we found that the set of spectral components was virtually identical for different values of the parameters N and p. The effects of forced vibrations under external electric fields of various types, including harmonic and pulsed periodic fields, observed in the total dipole moments of oligomer assemblies, were found to be similar in energy and spectral characteristics to those observed in single amino acid molecules.

Considering the typical selected spectral windows from the overview vibrational spectra of the oligomer assembly, computed from the total dipole moment, we observe a frequency proximity effect both among the local oscillators themselves and between these oscillators and the applied electric field. We can therefore assume that these windows exhibit effects of mutual coupling of local vibrations; such coupling is likely due to phonon interactions, leading to collective formation of spectral components. As the oligomer size increased, a redistribution of the spectral components was observed: the structure with two peaks in the center (at 3313.5 and 3358.1 cm^{-1}) was transformed into a structure with two peaks at 3277 and 3394.4 cm^{-1}. A similar evolution of spectral components was reproduced for other values of N. In our view, this effect is caused by Fermi resonance of the second harmonic of the vibrations at 1565.7 and 1695.5 cm^{-1} present in the spectrum, with the resonant frequency at 3333 cm^{-1}, which we were able to identify by applying an electric field.

No significant changes in the total dipole moment were observed for a single molecule under an applied electric field in the case of forced local vibrations, which likely points to conformational stability of a single oligomer upon excitation of local (rather than collective) vibrations. However, significant changes appear for larger numbers of oligomers in the assembly, when the parameter $p = 3$, 4, and 5. In this case, the effects of the applied electric field on intermolecular vibrations and dipole–dipole interactions may be observed.

During the simulation, a difference was revealed for the first time in the dependences of the resonance peaks of polyAlaN molecules at $N = 1$ and $N = 18$, on the electric field strength under square-wave excitation at a fundamental wavenumber of 3333 cm^{-1} (see Fig. 5). The resonance peak intensity is significantly higher for a single molecule (see Fig. 6) than for the oligomer, whose conformation and total energy are more stable with respect to excitation of intramolecular local oscillators.

Conclusion

We performed the first supercomputer molecular dynamics simulations of oligomers of several amino acids under electromagnetic fields in the IR range. The supercomputer methods developed here are suitable for applications in nanobiotechnology and microelectronics that incorporate biomolecular components, among which amino acid oligomers play a major role. The methodology has proven to be highly effective and reliable, yielding new results that consistently complement existing theoretical and experimental data. We used three types of amplitude modulation of the applied electric field (harmonic, a periodic sequence of unipolar rectangular pulses, and a symmetric square wave) to lay the groundwork for further practical studies and establish the means to monitor anharmonicity over a broad frequency band in the mid- and far-infrared regions.

The method allowed us to compare the frequency spectra of intrinsic molecular vibrations both in water and in the absence of a water environment, and to identify the common features and peculiarities. Adding water (*in silico*) shifted the frequencies upward by a few percent, i.e., towards higher vibrational energies. This shift likely originates from the specific intrinsic vibrational spectrum of water molecules, whose nonlinear couplings become active simultaneously with the local oscillators of the solutes.

A set of characteristics for both intrinsic local vibrational modes (normal modes) and forced vibrations of oligomers in the far- and mid-infrared ranges was identified for the first time. Interpretation of the obtained patterns allowed us to propose a consistent model of molecular physics, including mutual phonon couplings of local oscillators, satisfying the fundamental physical concepts of the intramolecular and intermolecular dynamics of groups of biomolecules.

The results can be used to determine the functional properties of dehydrated biomolecular films for applications in biophysics, nanobiotechnology, and microelectronics, for example in the design of prototypes of bioelectronic and heterogeneous hybrid microelectronic devices with embedded biomolecular components [55].

REFERENCES

1. **Ruan X., Ruan X., Huang H.,** Application of terahertz spectroscopy in medical microbiological detection, J. Phys. Conf. Ser. 2425 (1) 012045.

2. **Turton D. A., Senn H. M., Harwood T., et al.,** Terahertz underdamped vibrational motion governs protein-ligand binding in solution, Nat. Commun. 5 (03 Jun) (2014) 3999.

3. **Noble B. B., Todorova N., Yarovsky I.,** Electromagnetic bioeffects: A multiscale molecular simulation perspective, Phys. Chem. Chem. Phys. 24 (11) (2022) 6327–6348.

4. **Woods K. N.,** Solvent-induced backbone fluctuations and the collective librational dynamics of lysozyme studied by terahertz spectroscopy, Phys. Rev. E. 81 (3) (2010) 031915.

5. **Niehues G., Heyden M., Schmidt D. A., Havenith M.,** Exploring hydrophobicity by THz absorption spectroscopy of solvated amino acids, Faraday Discuss. 150 (23 May) (2011) 193–207.

6. **Jeong S.-Y., Cheon H., Lee D., Son J.-H.**, Determining terahertz resonant peaks of biomolecules in aqueous environment, Opt. Express. 28 (3) (2020) 3854–3863.

7. **Grechko M., Hasegawa T., D'Angelo F., et al.,** Coupling between intra- and intermolecular motions in liquid water revealed by two-dimensional terahertz-infrared-visible spectroscopy, Nat. Commun. 9 (1) (2018) 885.

8. **Xu J., Galan J., Ramian G., et al.,** Terahertz circular dichroism spectroscopy of biomolecules, In book: Jensen J. O., Theriault J.-M. (Eds.) Proc. SPIE. Vol. 5268: Chemical and Biological Standoff Detection. (27 Febr) (2004) 19–26.

9. **Beyer C., Christen P., Jelesarov I.**, **Fröhlichet J.,** Real-time assessment of possible electromagnetic-field-induced changesin protein conformation and thermal stability, Bioelectromagnetics. 35 (7) (2014) 470–478.

10. **Calabrò E., Magazщ S.,** Resonant interaction between electromagnetic fields and proteins: A possible starting point for the treatment of cancer, Electromagn. Biol. Med. 37 (3) (2018) 155–168.

11. **Harvey A.,** The interaction between electromagnetic fields at megahertz, gigahertz and terahertz frequencies with cells, tissues and organisms: Risks and potential, J. R. Soc. Interface. 14 (2017) 0585.

12. **Wu H., Ghaani M. R., Futera Z., English N. J.,** Effects of externally applied electric fields on the manipulation of solvated-chignolin folding: Static- versus alternating-field dichotomy at play, J. Phys. Chem. B. 126 (2) (2022) 376–386.

13. **Vaden T. D., de Boer T. S. J. A., Simons J. P., et al.,** Vibrational spectroscopy and conformational structure of protonated polyalanine peptides isolated in the gas phase, J. Phys. Chem. A. 112 (20) (2008) 4608–4616.

14. **Matsunaga Y., Koike R., Ota M., et al.,** Influence of structural symmetry on protein dynamics, PLoS One. 7 (11) (2012) e50011.

15. **Wako H., Endo S.,** Dynamic properties of oligomers that characterize low-frequency normal modes, Biophys. Physicobiol. 16 (Nov 29) (2019) 220–231.

16. **Husseini F. S., Robinson D., Hunt N. T., et al.,** Computing infrared spectra of proteins using the exciton model, J. Comput. Chem. 38 (16) (2017) 1362–1375.

17. **Schultheis V., Reichold R., Schropp B., Tavan P.,** A polarizable force field for computing the infrared spectra of the polypeptide backbone, J. Phys. Chem. B. 112 (39) (2008) 12217–12230.

18. **Narayan B., Herbert C., Rodriguez B. J., et al.,** Replica exchange molecular dynamics of diphenylalanine amyloid peptides in electric fields, J. Phys. Chem. B. 125 (20) (2021) 5233–5242.

19. **Bradshaw R. T., Dziedzic J., Skylaris Ch.-K., Essex J. W.,** The role of electrostatics in enzymes: Do biomolecular force fields reflect protein electric fields? J. Chem. Inf. Model. 60 (6) (2020) 3131–3144.

20. **Baranov M. A., Karseeva E. K., Tsybin O. Yu.,** Supercomputer simulation of intramolecular oscillations of glycine, diphenylalanine, and tryptophan in an electric field of the terahertz and infrared ranges, Biophysics. 69 (2) (2024) 179–194.

21. **Wolpert M., Hellwig P.,** Infrared spectra and molar absorption coefficients of the 20 alpha amino acids in aqueous solutions in the spectral range from 1800 to 500 cm^{-1}, Spectrochim. Acta A.: Mol. Biomol. Spectrosc. 64 (4) (2006) 987–1001.

22. **Barth A.,** Infrared spectroscopy of proteins, Biochim. Biophys. Acta Bioenerg. 1767 (9) (2007) 1073–1101.

23. **Zhang F., Tominaga K., Hayashi M., Wang H.-W.**, Low-frequency vibration study of amino acids using terahertz spectroscopy and solid-state density functional theory, In book: Zhang C., Zhang Xi-Ch., Nani M. (Eds.) Proc. SPI. Vol. 9275, Infrared, Millimeter-Wave, and Terahertz Technologies III; Conf.: SPIE/COS Photonics Asia 2014, 11 Nov., Beijing, P. 92750D.

24. **Moon J. H., Oh J. Y., Kim M. S.,** A systematic and efficient method to estimate the vibrational frequencies of linear peptide and protein ions with any amino acid sequence for the calculation of Rice-Ramsperger-Kassel-Marcus rate constant, J. Am. Soc. Mass Spectrom. 17 (12) (2006) 1749–1757.

25. **Baranov M. A., Shariaty F., Tsybin O. Y.** Dynamics of glycine, diphenylalanine, and tryptophan oligomers: Computer simulation in an IR electric field with different forms and polarization, J. Biomol. Struct. Dyn. 44 (5) (2026) 2651–2658.

26. **Barth A.,** The infrared absorption of amino acid side chains, Progr. Biophys. Mol. Biol. 74 (3–5) (2000) 141–173.

27. **Barth A., Zscherp C.,** What vibrations tell us about proteins, Q. Rev. Biophys. 35 (4) (2002) 369–430.

28. **Butyrskaya E. V., Nechaeva L. S., Shaposhnik V. A., Drozdova** E. **I.,** The assignment of the bands in IR spectra of aqueous solutions of glycine on the basis of quantum-chemical calculations, Sorbtsionnyye i Khromatograficheskiye Protsessy [Sorption & Chromatographic Processes]. 12 (4) (2012) 501–512 (in Russian).

29. **Redkov A. V., Osipov A. V., Kukushkin S. A.,** Molecular dynamics simulation of the indentation of nanoscale films on a substrate, Tech. Phys. Lett. 42 (6) (2016) 639–643.

30. **Nepomnyashchaya E. K., Baranov M. A., Tsybin O. Yu.,** Computer resonance dynamics of a glycine molecule in an infrared electric field, Pisma v Zhurnal Tekhnicheskoi Fiziki. 49 (7) (2023) 8 –11 (in Russian).

31. **Baranov M. A., Nepomnyashchaya E. K., Tsybin O. Yu.,** Fourier spectrum of the integral dipole moment of a number of amino acids supercomputer models, St. Petersburg State Polytechnical University Journal. Physics and Mathematics. 15 (4) (2022) 55–68 (in Russian).

32. **Baranov M. A., Tsybin O. Yu., Velichko E. N.,** Free energy relaxation of glycine, tryptophan and albumin molecules in the ionized aqueous solution: Computer analysis, St. Petersburg Polytechnical State University Journal. Physics and Mathematics. 14 (4) (2021) 135–146 (in Russian).

33. **Baranov M. A., Karseyeva E. K., Tsybin O. Yu.,** Supercomputer dynamical models of glycine, tryptophan and diphenyl-L-alanine in the electrical fields of terahertz and infrared spectral ranges, St. Petersburg State Polytechnical University Journal. Physics and Mathematics. 16 (3) (2023) 59–72 (in Russian).

34. **Goodsell D. S., Olson A. J.,** Structural symmetry and protein function, Annu. Rev. Biophys. Biomol. Struct. 29 (1) (2000) 105–153.

35. **Bahar I.**, **Lezon T. R., Bakan A., Shrivastava I. H.,** Normal mode analysis of biomolecular structures: Functional mechanisms of membrane proteins, Chem. Rev. 110 (3) (2010) 1463–1497.

36. **Faridoddin S., Baranov M. A., Tsybin O. Yu.,** Structure of biomolecular films through advanced imaging and statistical analysis, Colloids Surf. A. Physicoch. Eng. Asp. 702 (P. 1– 5 Dec) (2024) 134920.

37. **Kompan M. E., Baranov M. A., Malyshkin** V. G., **Tsybin O.Yu.,** Raman spectra in range 75 − 1200 cm^{-1} of amino acids L-tryptophan, diphenyl-L-alanine and glycine in aqueous solution and in dehydrated films, Phys. Solid State. 66 (8) (2024) 1445−1449 (in Russian).

38. **Löffler G., Schreiber H., Steinhauser O.,** Calculation of the dielectric properties of a protein and its solvent: Theory and a case study, J. Mol. Biol. 270 (3) (1997) 520−534.

39. **Baranov M., Tsybin O.,** Supercomputer simulation of amino acid molecules high-frequency polarizability in THz electric field, Proc. 2023 Int. Conf. on Electrical Engineering and Photonics (EExPolytech), 19−20 Oct., 2023, St. Petersburg, Russian Federation, IEEE (2023) 261−264.

40**. Karplus M.,** Molecular dynamics simulations of biomolecules, Acc. Chem. Res. 35 (6) (2002) 321−323.

41. **Ruiz M. P., Aragonиs A. C., Camarero N., et al.,** Bioengineering a single-protein junction, J. Am. Chem. Soc. 139 (43) (2017) 15337−15346.

42. **Reimann K., Woerner M., Elsaesser T.,** Two-dimensional terahertz spectroscopy of condensed-phase molecular systems, J. Chem. Phys. 154 (12) (2021) 120901.

43. **Solomentsev G. Y., English N. J., Mooney D. A.,** Effects of external electromagnetic fields on the conformational sampling of a short alanine peptide, J. Comput. Chem. 33 (9) (2012) 917−923.

44. **Kelly C. M., Northey T., Ryan K., et al.,** Conformational dynamics and aggregation behavior of piezoelectric diphenylalanine peptides in an external electric field, Biophys. Chem. 196 (Jan) (2015) 16−24.

45. **Hadley K. R., McCabe C.**, Coarse-grained molecular models of water: A review, Mol. Simul. 38 (8−9) (2012) 671−681.

46. **Mao Y., Zhang Y.,** Thermal conductivity, shear viscosity and specific heat of rigid water models, Chem. Phys. Lett. 542 (23 Jul) (2012) 37−41.

47. **MacKerell, Ir., A. D., Bashford D., Bellott M., et al.,** All-atom empirical potential for molecular modeling and dynamics studies of proteins, J. Phys. Chem. B. 102 (18) (1998) 3586−3616.

48**. Linstrom P. J., Mallard W. G.,** NIST standard reference database number 69, NIST (National Institute of Standards and Technologies) Chemistry WebBook. Vol. 1227. No. 69 (2005.) 20899.

49. **Feng J.-Y., Lee Y.-P., Zhu Ch.-Y., et al.,** IR−VUV spectroscopy of pyridine dimers, trimers and pyridine − ammonia complexes in a supersonic jet, Phys. Chem. Chem. Phys. 22 (37) (2020) 21520−21534.

50. **Zhang B.**, **Yu Y., Zhang Zh., et al.,** Infrared spectroscopy of neutral water dimer based on a tunable vacuum ultraviolet free electron laser, J. Phys. Chem. Lett. 11 (3) (2020) 851−855.

51. **Baranov M. A., Karseeva E. K., Tsybin O. Yu.,** Prototypes of devices for heterogeneous hybrid semiconductor electronics with an embedded biomolecular domain, Russian Microelectronics. 2023. Vol. 52 (6) (2023) 517−526.

СПИСОК ЛИТЕРАТУРЫ

1. **Ruan X., Ruan X., Huang H.** Application of terahertz spectroscopy in medical microbiological detection // Journal of Physics: Conference Series. 2022. Vol. 2425. No. 1. P. 012045.

2. **Turton D. A., Senn H. M., Harwood T., Lapthorn A. J., Ellis E. M., Wynne K.** Terahertz underdamped vibrational motion governs protein-ligand binding in solution // Nature Communications. 2014. Vol. 5. 03 June. P. 3999.

3. **Noble B. B., Todorova N., Yarovsky I.** Electromagnetic bioeffects: a multiscale molecular simulation perspective // Physical Chemistry Chemical Physics. 2022. Vol. 24. No. 11. Pp. 6327–6348.

4. **Woods K. N.** Solvent-induced backbone fluctuations and the collective librational dynamics of lysozyme studied by terahertz spectroscopy // Physical Review E. 2010. Vol. 81. No. 3. P. 031915.

5. **Niehues G., Heyden M., Schmidt D. A., Havenith M.** Exploring hydrophobicity by THz absorption spectroscopy of solvated amino acids // Faraday Discussions. 2011. Vol. 150. 23 May. Pp. 193–207.

6. **Jeong S.-Y., Cheon H., Lee D., Son J.-H.** Determining terahertz resonant peaks of biomolecules in aqueous environment // Optics Express. 2020. Vol. 28. No. 3. Pp. 3854–3863.

7. **Grechko M., Hasegawa T., D'Angelo F., Ito H., Turchinovich D., Nagata Y., Bonn M.** Coupling between intra- and intermolecular motions in liquid water revealed by two-dimensional terahertz-infrared-visible spectroscopy // Nature Communications. 2018. Vol. 9. No. 1. P. 885.

8. **Xu J., Galan J., Ramian G., Savvidis P., Scopatz A., Birge R. R., Allen S. J., Plaxco K.** Terahertz circular dichroism spectroscopy of biomolecules // Edited by Jensen J. O., Theriault J.-M. Proceedings SPIE. 2004. Vol. 5268. Chemical and Biological Standoff Detection. 27 February. Pp. 19–26.

9. **Beyer C., Christen P., Jelesarov I., Fröhlichet J.** Real-time assessment of possible electromagnetic-field-induced changesin protein conformationand thermal stability // Bioelectromagnetics. 2014. Vol. 35. No. 7. Pp. 470–478.

10. **Calabrò E., Magazщ S.** Resonant interaction between electromagnetic fields and proteins: A possible starting point for the treatment of cancer // Electromagnetic Biology and Medicine. 2018. Vol. 37. No. 3. Pp. 155–168.

11. **Harvey A.** The interaction between electromagnetic fields at megahertz, gigahertz and terahertz frequencies with cells, tissues and organisms: Risks and potential // Journal of the Royal Society, Interface. 2017. Vol. 14. P. 0585

12. **Wu H., Ghaani M. R., Futera Z., English N. J.** Effects of externally applied electric fields on the manipulation of solvated-chignolin folding: Static- versus alternating-field dichotomy at play // The Journal of Physical Chemistry B. 2022. Vol. 126. No. 2. Pp. 376–386.

13. **Vaden T. D., de Boer T. S. J. A., Simons J. P., Snoek L. C., Suhai S., Paizs B.** Vibrational spectroscopy and conformational structure of protonated polyalanine peptides isolated in the gas phase // The Journal of Physical Chemistry A. 2008. Vol. 112. No. 20. Pp. 4608–4616.

14. **Matsunaga Y., Koike R., Ota M., Tame J. R. H., Kidera A.** Influence of structural symmetry on protein dynamics // PLoS One. 2012. Vol. 7. No. 11. P. e50011.

15. **Wako H., Endo S.** Dynamic properties of oligomers that characterize low-frequency normal modes // Biophysics and Physicobiology. 2019. Vol. 16. November 29. Pp. 220–231.

16. **Husseini F. S., Robinson D., Hunt N. T., Parker A. W., Hirst J. D.** Computing infrared spectra of proteins using the exciton model // Journal of Computational Chemistry. 2017. Vol. 38. No. 16. Pp. 1362–1375.

17. **Schultheis V., Reichold R., Schropp B., Tavan P.** A polarizable force field for computing the infrared spectra of the polypeptide backbone // The Journal of Physical Chemistry B. 2008. Vol. 112. No. 39. Pp. 12217–12230.

18. **Narayan B., Herbert C., Rodriguez B. J., Brooks B. R., Buchete N.-V.**
Replica exchange molecular dynamics of diphenylalanine amyloid peptides in electric fields // The Journal of Physical Chemistry B. 2021. Vol. 125. No. 20. Pp. 5233–5242.

19. **Bradshaw R. T., Dziedzic J., Skylaris Ch.-K., Essex J. W.** The role of electrostatics in enzymes: Do biomolecular force fields reflect protein electric fields? // Journal of Chemical Information and Modeling. 2020. Vol. 60. No. 6. Pp. 3131–3144.

20. **Баранов М. А., Карсеева Э. К., Цыбин О. Ю.** Суперкомпьютерное моделирование внутримолекулярных колебаний глицина, дифенилаланина и триптофана в электрическом поле терагерцового и инфракрасного диапазонов // Биофизика. 2024. Т. 69. № 2. С. 213–229.

21. **Wolpert M., Hellwig P.** Infrared spectra and molar absorption coefficients of the 20 alpha amino acids in aqueous solutions in the spectral range from 1800 to 500 cm^{-1} // Spectrochimica Acta A.: Molecular and Biomolecular Spectroscopy. 2006. Vol. 64. No. 4. Pp. 987–1001.

22. **Barth A.** Infrared spectroscopy of proteins // Biochimica et Biophysica Acta – Bioenergetics. 2007. Vol. 1767. No. 9. Pp. 1073–1101.

23. **Zhang F., Tominaga K., Hayashi M., Wang H.-W.** Low-frequency vibration study of amino acids using terahertz spectroscopy and solid-state density functional theory // Zhang C., Zhang Xi-Ch., Nani M. (Eds.) Proceedings of SPI. Vol. 9275. Infrared, Millimeter-Wave, and Terahertz Technologies III. Conference: SPIE/COS Photonics Asia 2014. 11 November, Beijing, P. 92750D.

24. **Moon J. H., Oh J. Y., Kim M. S.** A systematic and efficient method to estimate the vibrational frequencies of linear peptide and protein ions with any amino acid sequence for the calculation of Rice-Ramsperger-Kassel-Marcus rate constant // Journal of the American Society for Mass Spectrometry. 2006. Vol. 17. No. 12. Pp. 1749–1757.

25. **Baranov M. A., Shariaty F., Tsybin O. Y.** Dynamics of glycine, diphenylalanine, and tryptophan oligomers: Computer simulation in an IR electric field with different forms and polarization // Journal of Biomolecular Structure and Dynamics. 2026. Vol. 44. No. 5. Pp. 2651–2658.

26. **Barth A.** The infrared absorption of amino acid side chains // Progress in Biophysics and Molecular Biology. 2000. Vol. 74. No. 3–5. Pp. 141–173.

27. **Barth A., Zscherp C.** What vibrations tell us about proteins // Quarterly Reviews of Biophysics. 2002. Vol. 35. No. 4. Pp. 369–430.

28. **Бутырская Е. В., Нечаева Л. С., Шапошник В. А., Дроздова В. И.** Отнесение полос в ИК спектрах водных растворов глицина на основе квантовохимического расчета // Сорбционные и хроматографические процессы. 2012. Т. 4 № .12. С. 512–501.

29. **Редьков А. В., Осипов А. В. Кукушкин С.А.** Моделирование процесса индентирования наномасштабных пленок на подложках методом молекулярной динамики // Письма в Журнал технической физики. 2016. Т. 42. № 12. С. 64–72.

30. **Непомнящая Э. К., Баранов М. А., Цыбин О. Ю.** Компьютерная резонансная динамика молекулы глицина в электрическом поле инфракрасного диапазона // Письма в Журнал технической физики. 2023. Т. 49. № 7. С. 8–11.

31. **Баранов М. А., Непомнящая Э. К., Цыбин О. Ю.** Фурье-спектр интегрального дипольного момента суперкомпьютерных моделей ряда аминокислот // Научно-технические ведомости СПбГПУ. Физико-математические науки. 2022. Т. 15. № 4. С. 55–68.

32. **Баранов М. А., Цыбин О. Ю., Величко Е. Н.** Компьютерный анализ релаксации свободной энергии молекул глицина, триптофана и альбумина в ионизованном водном растворе // Научно-технические ведомости СПбПУ. Физико-математические науки. 2021. Т. 14. № 4. С. 135–146.

33. **Баранов М. А., Карсеева Э. К., Цыбин О. Ю.** Суперкомпьютерные динамические модели глицина, триптофана и дифенилаланина в электрических полях терагерцового и инфракрасного спектральных диапазонов // Научно-технические ведомости СПбГПУ. Физико-математические науки. 2023. Т. 16. № 3. С. 59–72.

34. **Goodsell D. S., Olson A. J.** Structural symmetry and protein function // Annual Review of Biophysics and Biomolecular Structure. 2000. Vol. 29. No. 1. Pp. 105–153.

35. **Bahar I., Lezon T. R., Bakan A., Shrivastava I. H.** Normal mode analysis of biomolecular structures: Functional mechanisms of membrane proteins // Chemical Review. 2010. Vol. 110. No. 3. Pp. 1463–1497.

36. **Faridoddin S., Baranov M. A., Tsybin O. Yu.** Structure of biomolecular films through advanced imaging and statistical analysis // Colloids and Surfaces A: Physicochemical and Engineering Aspects. 2024. Vol. 702. Part 1. 5 December. P. 134920.

37. **Компан М. Е., Баранов М. А., Малышкин В. Г., Цыбин О. Ю.** Спектры комбинационного рассеяния в диапазоне 1200 – 75 $см^{-1}$ аминокислот L-триптофана, дифенил-L-аланина и глицина в водном растворе и в гидратированных пленках // Физика твердого тела. 2024. Т. 66. № 8. С. 1445–1449.

38. **Löffler G., Schreiber H., Steinhauser O.** Calculation of the dielectric properties of a protein and its solvent: Theory and a case study // Journal of Molecular Biology. 1997. Vol. 270. No. 3. Pp. 520–534.

39. **Baranov M., Tsybin O.** Supercomputer simulation of amino acid molecules high-frequency polarizability in THz electric field // Proceedings of the 2023 International Conference on Electrical Engineering and Photonics (EExPolytech), 19–20 October 2023. St. Petersburg, Russian Federation. IEEE, 2023. Pp. 261–264.

40**. Karplus M.** Molecular dynamics simulations of biomolecules // Accounts of Chemical Research. 2002. Vol. 35. No. 6. Pp. 321–323.

41. **Ruiz M. P., Aragonиs A. C., Camarero N., Vilhena J. G., Ortega M., Zotti L. A., Pérez R., Cuevas J. C., Gorostiza P., Днez-Pérez I.** Bioengineering a single-protein junction // Journal of the American Chemical Society. 2017. Vol. 139. No. 43. Pp. 15337–15346.

42. **Reimann K., Woerner M., Elsaesser T.** Two-dimensional terahertz spectroscopy of condensed-phase molecular systems // The Journal of Chemical Physics. 2021. Vol. 154. No. 12. P. 120901.

43. **Solomentsev G. Y., English N. J., Mooney D. A.** Effects of external electromagnetic fields on the conformational sampling of a short alanine peptide // Journal of Computational Chemistry. 2012. Vol. 33. No. 9. Pp. 917–923.

44. **Kelly C. M., Northey T., Ryan K., Brooks B. R., Kholkin A. L., Rodriguez B. J., Buchete N.-V.** Conformational dynamics and aggregation behavior of piezoelectric diphenylalanine peptides in an external electric field // Biophysical Chemistry. 2015. Vol. 196. January. Pp. 16–24.

45. **Hadley K. R., McCabe C.** Coarse-grained molecular models of water: A review // Molecular Simulation. 2012. Vol. 38. No. 8–9. Pp. 671–681.

46. **Mao Y., Zhang Y.** Thermal conductivity, shear viscosity and specific heat of rigid water models // Chemical Physics Letters. 2012. Vol. 542. 23 July. Pp. 37–41.

47. **MacKerell, Ir., A. D., Bashford D., M. Bellott M., et al.** All-atom empirical potential for molecular modeling and dynamics studies of proteins // The Journal of Physical Chemistry B. 1998. Vol. 102. No. 18. Pp. 3586–3616.

48**. Linstrom P. J., Mallard W. G.** NIST standard reference database number 69 // NIST (National Institute of Standards and Technologies) Chemistry WebBook. 2005. Vol. 1227. No. 69. P. 20899.

49. **Feng J.-Y., Lee Y.-P., Zhu Ch.-Y., Hsu P.-J., Kuo J.-L., Ebata T.** IR–VUV spectroscopy of pyridine dimers, trimers and pyridine – ammonia complexes in a supersonic jet // Physical Chemistry Chemical Physics. 2020. Vol. 22. No. 37. Pp. 21520–21534.

50. **Zhang B.**, **Yu Y., Zhang Zh., et al.** Infrared spectroscopy of neutral water dimer based on a tunable vacuum ultraviolet free electron laser // The Journal of Physical Chemistry Letters. 2020. Vol. 11. No. 3. Pp. 851–855.

51. **Баранов М. А., Карсеева Е. К., Цыбин О. Ю.** Прототипы приборов гетерогенной гибридной полупроводниковой электроники с встроенным биомолекулярным доменом // Микроэлектроника. 2023. Т. 52. № 6. Р. 497–507.

THE AUTHORS

BARANOV Maksim A.
Peter the Great St. Petersburg Polytechnic University
29 Politechnicheskaya St., St. Petersburg, 195251, Russia
baranovma1993@gmail.com
ORCID: 0000-0003-4555-0009

TSYBIN Oleg Yu.
Peter the Great St. Petersburg Polytechnic University
29 Politechnicheskaya St., St. Petersburg, 195251, Russia
oleg.tsybin@gmail.com
ORCID: 0000-0002-8308-059X

СВЕДЕНИЯ ОБ АВТОРАХ

БАРАНОВ Максим Александрович – *кандидат физико-математических наук, доцент Высшей школы прикладной физики и космических технологий Санкт-Петербургского политехнического университета Петра Великого.*
195251, Россия, г. Санкт-Петербург, Политехническая ул., 29
baranovma1993@gmail.com
ORCID: 0000-0003-4555-0009

ЦЫБИН Олег Юрьевич – *доктор физико-математических наук, профессор Высшей школы прикладной физики и космических технологий Санкт-Петербургского политехнического университета Петра Великого.*
195251, Россия, г. Санкт-Петербург, Политехническая ул., 29
oleg.tsybin@gmail.com
ORCID: 0000-0002-8308-059X

Received 24.04.2025. Approved after reviewing 27.02.2026. Accepted 27.02.2026.
Статья поступила в редакцию 24.04.2025. Одобрена после рецензирования 27.02.2026. Принята 27.02.2026.

© Peter the Great St. Petersburg Polytechnic University, 2026